Journal of Statistical Physics, Vol. 88, Nos. 5/6, 1997

Continuum Percolation of the Four-Bonding-Site Associating Fluids

Eduard Vakarin,[1] Yurko Duda,[2,3] and Myroslav Holovko[1]

Received November 13, 1996; final March 3, 1997

Wertheim's integral equation theory for associating fluids is reformulated for the study of the connectedness properties of associating hard spheres with four bonding sites. The association interaction is described as a square-well saturable attraction between these sites. The connectedness version of the Ornstein–Zernike (OZ) integral equation is supplemented by the PY-like closure relation and solved analytically within an ideal network approximation in which the network is represented as resulting from the crossing of ideal polymer chains. The pair connectedness functions and the mean cluster size are calculated and discussed. The condition for the percolation transition and the analytical form of the percolation threshold are derived. The connection of the percolation with the gas–liquid phase transition is discussed.

KEY WORDS: Percolation; association; integral equation; ideal network.

1. INTRODUCTION

Percolation concept is a subject common to many problems connected with the determination of macroscopic properties which are strongly affected by the appearing of an infinite cluster.[1] These proccesses include the sol–gel transition in polymerizing systems,[2] conductivity and transport phenomena in porous and disordered media, particle aggregation in colloids,[3] microemulsions and suspensions.

Systematical investigation of the continuum percolation within the integral equation theory has been initiated by Coniglio *et al.*,[4] who have derived the connectedness analog of usual OZ integral equation. Based on

[1] Institute for Condensed Matter Physics, Lviv 11, Ukraine.
[2] Instituto de Química de la UNAM, Circuito Exterior, Coyoacán 04510, México D.F., Mexico.
[3] Permanent address: Institute for Condensed Matter Physics, Lviv 11, Ukraine.

0022-4715/97/0900-1333$12.50/0 © 1997 Plenum Publishing Corporation

822/88/5-6-22

this the connectivity of the systems with central attractive potentials including permeable and adhesive spheres,[5] randomly centered and permeable spheres,[6–8] extended hard spheres,[9] hard core Yukawa fluids,[10] square-well fluids[11] has been investigated.

The percolation properties of the so-called associating fluids have been studied also. Clustering and gelation in dimerizing fluids have been discussed in refs. 12, 13. In particular, the dimerizing sticky hard sphere model has been shown to be useful in a description of the percolation in micellar microemulsions with dissolved protein.[13, 14] Connectivity in chain-like fluids have been studied in refs. 15, 16 by means of RISM and also in ref. 17 within the Wertheim's associative approach.[18–21] The evidence of the percolation behavior in network-forming systems has been given in the works of Stanley, Teixeira *et al.*,[22–24] where the molecular dynamics study of the ST2 model of water is discussed.

The above studies have been concerned with the potential models consisting of two parts. First of them has been chosen to be an associating saturable interaction, responsible for a formation of finite size aggregates. The second part has been represented by a spherically symmetric (say, adhesive or square well) attraction responsible for the percolation. The association has been detected to cause a shift of the percolation threshold with respect to nonassociating system.

The aim of the present paper is to study the clustering due to the associating potential only. This problem is different in principle from those mentioned above. In fact, we are going to examine how a growing cluster can be built up of monomeric omits due to covalent bonds. In particular, we consider the four bonding site model of associating fluids. Thermodynamic and structural properties of this model have been studied in refs. 25, 27. The site-site interaction in this case may cause the formation of network complexes. Our purpose is to study the conditions at which the network appears as an infinite cluster. For this aim we reformulate the Wertheim's integral equation theory and solve the connectivity Ornstein–Zernike (OZ) equation within the PY approximation. Similar scheme has been developed in ref. 17 for the analysis of the connectivity in polymerizing fluids. In addition we adapt here an ideal network approximation[27] in which the network is described as a tree-like structure where there is only single path of associative bonds between any pair of molecules. We obtain analytically the mean cluster size, the condition for the percolation threshold, and, finally, the pair connectedness functions for the model under consideration. We discuss also a relation between the gas–liquid transition and the percolation threshold. The liquid is shown to lie inside the percolation region. This allows us to conclude that the liquid state (for the model) results from the condensation of an infinite network.

2. PERCOLATION CONCEPT WITHIN THE MULTIDENSITY FORMALISM

We consider the system of hard spheres of number density ρ with each sphere containing four embedded attractive sites, denoted as A, B, C, D. The hard core diameter is denoted as d. The sites are randomly located at the surface of each sphere and assumed to be independent of each other. This means that the bonded state of a given site does not affect the bonding at the other sites of the same molecule. Only AC, BC, AD and BD bonding between different molecules are allowed. For the following analysis we will follow the notations introduced by Wertheim.[19] The superscripts F or F' denote the sites C and D, the subscripts G or G' stand for the sites A and B. The lower symbol Γ denotes the state with two bonded A and B sites on the same sphere. The upper symbol Γ has similar meaning with respect to C and D sites. For the derivation of basic relations we suppose that the system is affected by a virtual one particle potential which will be taken as zero in actual calculations. The detailed analysis of the structural and thermodynamic properties of this model has been presented in our previous work.[27]

The pair potential consists of the blocked and connectedness parts:

$$U(1,2) = U^*(1,2) + U^\dagger(1,2) \tag{1}$$

The connectedness part is the sum of association contributions

$$U^\dagger(1,2) = \sum_{G,F} U_G{}^F(1,2) + \sum_{G,F} U^F{}_G(1,2) \tag{2}$$

where $U^*(1,2)$ is the blocked part which is not responsible for the clusterization and represents the interaction of the molecules not connected into a cluster, it is modelled by the hard sphere potential. $U_G{}^F(1,2)$ denotes the potential for a short-ranged and highly directional attractive force between site G on molecule 1 and site F on molecule 2. The attraction between site F of molecule 1 and site G of molecule 2 is described by the value $U^F{}_G(1,2)$. The association potential is given in the square well form:

$$U_G{}^F(1,2) = U^F{}_G(1,2) = \begin{cases} -E_G^F; & x_G^F < x_c \\ 0; & x_G^F \geqslant x_c \end{cases} \tag{3}$$

Here x_G^F is the distance between the sites F and G of the molecules 1 and 2, E_G^F is the depth and x_c is the width of the potential well.

The Mayer function can be expressed as:

$$f(1,2) = f^*(1,2) + f^\dagger(1,2) \tag{4}$$

with the connectedness part being defined as

$$f^{\dagger}(1,2) = e^{*}(1,2) \sum_{G,F} \Bigg[f_G{}^F(1,2) + f^F{}_G(1,2) + \prod_{i,\alpha=G',F'}^{G,F} [f_i^{\alpha}(1,2) + f^{\alpha}{}_i(1,2)] \Bigg] \tag{5}$$

Here, $e^{*}(1,2) = \exp\{-\beta U^{*}(1,2)\}$ and $f_G{}^F(1,2) = \exp\{-\beta U_G{}^F(1,2)\} - 1$. The last term in the bracket of equation (5) represents the multiple bonding between the molecules labeled as 1 and 2. For the short-ranged part of the potential, this term will be neglected due to the steric saturation condition which imposes a restriction on the association potential. Note that the connectedness Mayer function $f^{\dagger}(1,2)$ is defined here to be different from the exponential of $U^{\dagger}(1,2)$, as it was proposed in.[4,5] A division of the Mayer function onto the blocked and connectedness parts is, to some extent, arbitrary. The only restriction is that the equation (4) is satisfied consistently with the division (1) of the potential. The above choice for $f^{\dagger}(1,2)$ is motivated by our purpose to reduce the percolation problem to the starting point of the association theory. According to the multidensity formalism developed by Wertheim,[19] the pair correlation functions are described by the associative OZ integral equation:

$$h_{i,j}^{\alpha,\beta}(1,2) = c_{i,j}^{\alpha,\beta}(1,2) + \sum_{l,m} \sum_{\gamma,\varepsilon} \int d(3)\, c_{i,l}^{\alpha,\gamma}(1,3)\, \sigma_{\Gamma-l-m}^{\Gamma-\gamma-\varepsilon}(3)\, h_{m,j}^{\varepsilon,\beta}(3,2) \tag{6}$$

Here, the indexes $\{i, j, l, m\}$ and $\{\alpha, \beta, \gamma, \varepsilon\}$ are assigned the values 0, G, Γ and 0, F, Γ respectively.

For the analysis of the connectivity properties we extract from each correlation function the subset of graphs which contain at least one unbroken path of f_G^F bonds between the root points.

$$\begin{aligned} h_{i,j}^{\alpha,\beta}(1,2) &= h_{i,j}^{\alpha,\beta\dagger}(1,2) + h_{i,j}^{\alpha,\beta}{}^{*}(1,2), \\ c_{i,j}^{\alpha,\beta}(1,2) &= c_{i,j}^{\alpha,\beta\dagger}(1,2) + c_{i,j}^{\alpha,\beta}{}^{*}(1,2) \end{aligned} \tag{7}$$

The connectedness pair and direct correlation functions satisfy the OZ integral equation

$$h_{i,j}^{\alpha,\beta\dagger}(1,2) = c_{i,j}^{\alpha,\beta\dagger}(1,2) + \sum_{l,m} \sum_{\gamma,\varepsilon} \int d(3)\, c_{i,l}^{\alpha,\gamma\dagger}(1,3)\, \sigma_{\Gamma-l-m}^{\Gamma-\gamma-\varepsilon}(3)\, h_{m,j}^{\varepsilon,\beta\dagger}(3,2) \tag{8}$$

For the sake of clarity it is useful to rearrange equation (8) in the matrix form:

$$\mathbf{h}^{\dagger}(1,2)=\mathbf{c}^{\dagger}(1,2)+\int d(3)\,\mathbf{c}^{\dagger}(1,3)\,\boldsymbol{\sigma}(3)\,\mathbf{h}^{\dagger}(3,2) \tag{9}$$

where the matrices are defined as follows:

$$\mathbf{c}^{\dagger}(1,2)=\begin{bmatrix} \hat{c}^{\dagger}_{00} & \hat{c}^{\dagger}_{0A} & \hat{c}^{\dagger}_{0B} & \hat{c}^{\dagger}_{A\Gamma} \\ \hat{c}^{\dagger}_{A0} & \hat{c}^{\dagger}_{AA} & \hat{c}^{\dagger}_{AB} & \hat{c}^{\dagger}_{A\Gamma} \\ \hat{c}^{\dagger}_{B0} & \hat{c}^{\dagger}_{BA} & \hat{c}^{\dagger}_{BB} & \hat{c}^{\dagger}_{B\Gamma} \\ \hat{c}^{\dagger}_{\Gamma 0} & \hat{c}^{\dagger}_{\Gamma A} & \hat{c}^{\dagger}_{\Gamma B} & \hat{c}^{\dagger}_{\Gamma\Gamma} \end{bmatrix}; \qquad \mathbf{h}^{\dagger}(1,2)=\begin{bmatrix} \hat{h}^{\dagger}_{00} & \hat{h}^{\dagger}_{0A} & \hat{h}^{\dagger}_{0B} & \hat{h}^{\dagger}_{A\Gamma} \\ \hat{h}^{\dagger}_{A0} & \hat{h}^{\dagger}_{AA} & \hat{h}^{\dagger}_{AB} & \hat{h}^{\dagger}_{A\Gamma} \\ \hat{h}^{\dagger}_{B0} & \hat{h}^{\dagger}_{BA} & \hat{h}^{\dagger}_{BB} & \hat{h}^{\dagger}_{B\Gamma} \\ \hat{h}^{\dagger}_{\Gamma 0} & \hat{h}^{\dagger}_{\Gamma A} & \hat{h}^{\dagger}_{\Gamma B} & \hat{h}^{\dagger}_{\Gamma\Gamma} \end{bmatrix} \tag{10}$$

The density matrix is of usual form:[27]

$$\boldsymbol{\sigma}=\begin{bmatrix} \hat{\sigma}_{\Gamma} & \hat{\sigma}_{B} & \hat{\sigma}_{A} & \hat{\sigma}_{0} \\ \hat{\sigma}_{B} & \hat{0} & \hat{\sigma}_{0} & \hat{0} \\ \hat{\sigma}_{A} & \hat{\sigma}_{0} & \hat{0} & \hat{0} \\ \hat{\sigma}_{0} & \hat{0} & \hat{0} & \hat{0} \end{bmatrix} \tag{11}$$

These matrices are obtained from those written in usual equation (6) by excluding the correlation functions inconsistent with the connectedness condition. For instance, the functions $h^{00\dagger}_{00}(1,2)$ or $h^{0G\dagger}_{0F}(1,2)$ vanish since the labeled point 1 has not an associative bond. The submatrices are defined in a similar manner.[27] In particular, we have

$$\hat{c}^{\dagger}_{00}(1,2)=\begin{bmatrix} 0 & 0 & 0 & 0 \\ 0 & c^{CC\dagger}_{00} & c^{CD\dagger}_{00} & c^{C\Gamma\dagger}_{00} \\ 0 & c^{DC\dagger}_{00'} & c^{DD\dagger}_{00} & c^{D\Gamma\dagger}_{00} \\ 0 & c^{\Gamma C\dagger}_{00} & c^{\Gamma D\dagger}_{00} & c^{\Gamma\Gamma\dagger}_{00} \end{bmatrix}$$

$$\hat{h}^{\dagger}_{00}(1,2)=\begin{bmatrix} 0 & 0 & 0 & 0 \\ 0 & h^{CC\dagger}_{00} & h^{CD\dagger}_{00} & h^{C\Gamma\dagger} \\ 0 & h^{DC\dagger}_{00'} & h^{DD\dagger}_{00} & h^{D\Gamma\dagger}_{00} \\ 0 & h^{\Gamma C\dagger}_{00} & h^{\Gamma D\dagger}_{00} & h^{\Gamma\Gamma\dagger}_{00} \end{bmatrix} \tag{12}$$

$$\hat{c}^{\dagger}_{GG'}(1,2)=\begin{bmatrix} c^{00\dagger}_{GG'} & c^{0C\dagger}_{GG'} & c^{0D\dagger}_{GG'} & c^{0\Gamma\dagger}_{GG'} \\ c^{C0\dagger}_{GG'} & c^{CC\dagger}_{GG'} & c^{CD\dagger}_{GG'} & c^{C\Gamma\dagger}_{GG'} \\ c^{D0\dagger}_{GG'} & c^{DC\dagger}_{GG'} & c^{DD\dagger}_{GG'} & c^{D\Gamma\dagger}_{GG'} \\ c^{\Gamma 0\dagger}_{GG'} & c^{\Gamma C\dagger}_{GG'} & c^{\Gamma D\dagger}_{GG'} & c^{\Gamma\Gamma\dagger}_{GG'} \end{bmatrix}$$

$$\hat{h}^{\dagger}_{GG'}(1,2)=\begin{bmatrix} h^{00\dagger}_{GG'} & h^{0C\dagger}_{GG'} & h^{0D\dagger}_{GG'} & h^{0\Gamma\dagger}_{GG'} \\ h^{C0\dagger}_{GG'} & h^{CC\dagger}_{GG'} & h^{CD\dagger}_{GG'} & h^{C\Gamma\dagger}_{GG'} \\ h^{D0\dagger}_{GG'} & h^{DC\dagger}_{GG'} & h^{DD\dagger}_{GG'} & h^{D\Gamma\dagger}_{GG'} \\ h^{\Gamma 0\dagger}_{GG'} & h^{\Gamma C\dagger}_{GG'} & h^{\Gamma D\dagger}_{GG'} & h^{\Gamma\Gamma\dagger}_{GG'} \end{bmatrix} \tag{13}$$

The density submatrices are:

$$\hat{\boldsymbol{\sigma}}_{\Gamma}=\begin{bmatrix} \sigma^{\Gamma}_{\Gamma} & \sigma^{D}_{\Gamma} & \sigma^{C}_{\Gamma} & \sigma^{0}_{\Gamma} \\ \sigma^{D}_{\Gamma} & 0 & \sigma^{0}_{\Gamma} & 0 \\ \sigma^{C}_{\Gamma} & \sigma^{0}_{\Gamma} & 0 & 0 \\ \sigma^{0}_{\Gamma} & 0 & 0 & 0 \end{bmatrix}, \qquad \hat{\boldsymbol{\sigma}}_{G}=\begin{bmatrix} \sigma^{\Gamma}_{G} & \sigma^{D}_{G} & \sigma^{C}_{G} & \sigma^{0}_{G} \\ \sigma^{D}_{G} & 0 & \sigma^{0}_{G} & 0 \\ \sigma^{C}_{G} & \sigma^{0}_{G} & 0 & 0 \\ \sigma^{0}_{G} & 0 & 0 & 0 \end{bmatrix},\ldots \tag{14}$$

All the matrices required could be obtained within the recipe described above by the appropriate substitution of the indices. Here, the values σ^{j}_{i} are the combinations of the partial densities ρ^{β}_{α} which account for a bonded state of the sites.

$$\sigma^{\alpha}_{i}(1)=\sum_{j=0}^{i}\sum_{\beta=0}^{\alpha}\varrho^{\beta}_{j}(1) \tag{15}$$

Equation (8) should be supplemented by a closure relation. We propose the following PY-like closure:

$$c^{\alpha,\beta\dagger}_{i,j}(1,2)=f^{*}(1,2)\,y^{\alpha,\beta\dagger}_{i,j}(1,2) + e^{*}(1,2)\sum_{F,G}\left[f^{F}_{G}(1,2)\,y^{\alpha-F,\beta}_{i,j-G}(1,2)+f_{G}{}^{F}(1,2)\,y^{\alpha,\beta-F}_{i-G,j}(1,2)\right] \tag{16}$$

where the connectedness cavity correlation function $y^{\alpha,\beta\dagger}_{i,j}(1,2)$ is defined by

$$g^{\alpha,\beta\dagger}_{i,j}(1,2)=h^{\alpha,\beta\dagger}_{i,j}(1,2)=e^{*}(1,2)\,y^{\alpha,\beta\dagger}_{i,j}(1,2) + e^{*}(1,2)\sum_{F,G}\left[f^{F}_{G}(1,2)\,y^{\alpha-F,\beta}_{i,j-G}(1,2)+f_{G}{}^{F}(1,2)\,y^{\alpha,\beta-F}_{i-G,j}(1,2)\right] \tag{17}$$

Here the singular, i.e. including the $f_G^F(1,2)$, part describes the direct correlation between two points in the same cluster, while the regular part corresponds to the indirect correlation. We thus see that the relations (8)–(17) do not form a closed set since the connectedness functions are expressed through the partial functions $g_{i,j}^{\alpha,\beta}(1,2)$. A solution of the OZ equation (6) is, therefore, required.

The total connectedness correlation function is the following superposition of the partial functions:

$$\varrho(1)\, g^{\dagger}(1,2)\, \varrho(2) = \sum_{i,j} \sum_{\alpha,\beta} \sigma_i^{\alpha}(1)\, g_{\Gamma-i,\Gamma-j}^{\Gamma-\alpha,\Gamma-\beta\dagger}(1,2)\, \sigma_j^{\beta}(2) \tag{18}$$

The most important measure of the connectedness is the mean cluster size S given by

$$S = 1 + \frac{\rho}{V} \int d1\, d2 g^{\dagger}(1,2) \tag{19}$$

where V is the sample volume. As the percolation transition is approached S increases and becomes infinite at the percolation threshold.

3. THE IDEAL NETWORK APPROXIMATION

In the previous section we have developed a general scheme for investigation of the connectivity properties within the association concept. The model under consideration can be used for a description of linear polymers, symmetrical and nonsymmetrical networks. The network may consist of very complicated aggregates (e.g. linear branches, loops, crossing rings, etc.) which require more and more refined description. As a first step we neglect the formation of ring-like structures and describe the network as a singly connected structure (like the Cayley tree). This is the ideal network approximation[27] which is based on following assumptions. We neglect all the graphs in $\varrho(1)$ which contain the intramolecular (s-mer) subgraphs corresponding to $s \geqslant 3$. This restriction is valid for each GF pair of bonded sites and corresponds to the dimer approximation for each of GF bonds. In other words, we assume that only one bond at any association site is allowed. This means that the association potential (3) is regarded to be short ranged enough to involve the steric saturation condition. In addition we take into account the possibility of only single bonding between the molecules. Thus, we neglect any diagrammatic series in $\varrho(1)$ with the multiple bonded labeled point included into a ring graph. Those statements result in the following relation amongst the partial densities

$$\frac{\sigma_I^I(1)}{\sigma_G^I(1)} = \frac{\sigma_I^F(1)}{\sigma_G^F(1)} = \frac{\sigma_I^0(1)}{\sigma_G^0(1)} = m_{I-G}(1) \tag{20}$$

$$\frac{\sigma_I^I(1)}{\sigma_I^F(1)} = \frac{\sigma_G^I(1)}{\sigma_G^F(1)} = \frac{\sigma_0^I(1)}{\sigma_0^F(1)} = m^{I-F}(1) \tag{21}$$

As we have discussed earlier[27] the values $m_G(1)$ and $m_F(1)$ can be identified with characteristics of association in a labeled point, but cannot be regarded to describe the size of the aggregates. This is in contrast to the two site polymer chains case[31] where m is the mean chain length.

Physically, our system can be viewed as that consisting of cross-like aggregates with each one being formed by the branches crossing at a common molecule. In our case we neglect the part of the intramolecular correlation responsible for the formation of the ring-like complexes with respect to all GF pairs of the sites. Thus, the network may consist of crossing polymer chains built along each of AC, AD, BC, BD directions, with each polymer branch being described within the ideal chain approximation.[31] It is important that the structure is tree-like, i.e. there is no selfcrossing of the branches. Any pair of molecules in such a network is assumed to remain singly connected with changing density and association.

The relation amongst the densities can also be represented in terms of the fractions $X_G(1)$ and $X_F(1)$ of the molecules not bonded at sites G and F respectively:

$$X_G(1) + X_G(1) \sum_F \int d(2)\, g_{00}^{00}(1, 2)\, f_G{}^F(1, 2)\, \varrho(2)\, X^F(2) = 1 \tag{22}$$

$$X_F(1) + X^F(1) \sum_G \int d(2)\, g_{00}^{00}(1, 2)\, f^F{}_G(1, 2)\, \varrho(2)\, X_G(2) = 1 \tag{23}$$

Here $\varrho(1)\, X_G(1) = \sigma_{I-G}^I(1)$ and $\varrho(1)\, X^F(1) = \sigma_I^{I-F}(1)$. We note that the above relations amongst the densities are identical to those obtained in the framework of thermodynamic perturbation theory.[19, 25, 26] In the case of energetically equivalent sites (i.e $X^F(1) = X_G(1) = X_A(1)$) the relations (22), (23) allow one to define χ_n, the fractions of the molecules bonded at n sites[25, 26]

$$\chi_0(1) = X_A^4(1) \tag{24}$$

$$\chi_1(1) = 4X_A^3(1)[1 - X_A(1)] \tag{25}$$

$$\chi_2(1) = 6X_A^2(1)[1 - X_A(1)]^2 \tag{26}$$

$$\chi_3(1) = 4X_A(1)[1 - X_A(1)]^3 \tag{27}$$

$$\chi_4(1) = [1 - X_A(1)]^4 \tag{28}$$

The average member of bonds n_b per molecule can be calculated as:[24]

$$n_b(1) = \sum_{k=1}^{4} k\chi_k(i) = 4[1 - X_A(1)] \tag{29}$$

The connectivity OZ equation (8) can also be simplified, since the only functions $h_{G0}^{0F\dagger}(1,2)$ or $h_{0G}^{F0\dagger}(1,2)$ and $h_{GG'}^{00\dagger}$ or $h_{00}^{FF'}(1,2)$ survive within the ideal network approximation. In the case of equivalent sites we have two fixations: the singular $h_s^\dagger = \{h_{G0}^{0F\dagger}, h_{0G}^{F0\dagger}\}$ and the regular $h_r^\dagger = \{h_{GG'}^{00\dagger}, h_{00}^{FF'\dagger}\}$. Then the connectivity OZ equation can be reduced to the following lower dimension matrix form

$$h_{i,j}^\dagger(1,2) = c_{i,j}^\dagger(1,2) + \sum_{l,m} \int d3 c_{il}^\dagger(1,3)\, \sigma_{lm}(3)\, h_{mj}^\dagger(3,2) \tag{30}$$

where the matrices are defined as

$$\mathbf{h}^\dagger = \begin{bmatrix} h_s^\dagger & h_r^\dagger \\ h_r^\dagger & h_s^\dagger \end{bmatrix}, \qquad \mathbf{c}^\dagger = \begin{bmatrix} c_s^\dagger & c_r^\dagger \\ c_r^\dagger & c_s^\dagger \end{bmatrix}, \qquad \boldsymbol{\sigma} = \begin{bmatrix} 4\sigma_2 & 2\sigma_2 \\ 2\sigma_2 & 4\sigma_2 \end{bmatrix} \tag{31}$$

and $\sigma_2 = \rho X_A^2$.

The PY-like closure relation (16) takes the form

$$c_s^\dagger(1,2) = f^*(1,2)\, y_s^\dagger(1,2) + e^*(1,2)[f_{as}(1,2)\, y_{00}^{00}(1,2)] \tag{32}$$

$$c_r^\dagger(1,2) = f^*(1,2)\, y_r^\dagger(1,2) \tag{33}$$

where $y_s^\dagger(1,2)$ and $y_r^\dagger(1,2)$ are defined from

$$g_s^\dagger(1,2) = e^*(1,2)\, y_s^\dagger(1,2) + e^*(1,2)[f_{as}(1,2)\, y_{00}^{00}(1,2)] \tag{34}$$

$$g_r^\dagger(1,2) = e^*(1,2)\, y_r^\dagger(1,2) \tag{35}$$

Here, $f_{as}(1,2) = f_G{}^F(1,2) = f^F{}_G(1,2)$. The total connectedness function is the following combination of the regular and singular parts:

$$g^\dagger(1,2) = 8X_A(1)\, X_A(2)[g_s^\dagger(1,2) + g_r^\dagger(1,2)] \tag{36}$$

4. STICKY LIMIT AND FACTORIZATION

The scheme described above is applicable to a study of the connectivity properties of an inhomogeneous system with the strongly directional associative potential. We shall consider a spatially homogeneous system and assume that the pair quantities depend on the distance r between the

centres of two molecules and on their orientations. The one-particle densities are independent of the position of a given molecule. Since the sites G, F are assumed to be randomly located on the surface of each molecule, there is no restriction on the orientation of the sites. Therefore we consider the orientation averaged values for the association:

$$f_G{}^F(r) = \frac{1}{\Omega^2} \int f_G{}^F(1, 2)\, d\omega_{1,G}\, d\omega_{1,F}\, d\omega_{2,G}\, d\omega_{2,F} \tag{37}$$

where $\omega_{1,G}$ and $\omega_{1,F}$ denote the orientation of the sites G and F of molecule 1 and Ω is the normalization constant. Here, the integration over the orientations of two molecules is equivalent to the integration over the sites orientation, since the sites are assumed to be independent of each other. We note that the procedure of the orientation averaging eliminate the angular dependence of the pairwise quantities, but the steric incompatibility does reflect the strongly directional character of the associative interaction.

To provide an analytical treatment of the present model we follow Baxter[36] and substitute the square-well attractive potential by its limiting case: infinitely narrow and infinitely deep potential under the constraint that the second virial coefficient for the association potential is kept constant.

In this limit the Mayer function (5) is given by

$$f_G{}^F(r) = f^F{}_G(r) = K_G^F\, \delta(r - d) \tag{38}$$

where K_G^F are the parameters for the strength of association. Note, however, that the above substitution does not mean a direct replacement of association potential by a spherically symmetric sticky potential. We just replace the square-well site–site attraction by a δ-like one. The highly directional nature of the association is reflected by the bonded state indices which obey the steric saturation condition. The model is, therefore, different from that of Baxter,[36] even when orientation averaged quantities are involved into consideration.

As is already mentioned we consider here a symmetrical network with equivalent sites (i.e. $K_G^F = K$). Thus, the theory proposed is independent, of the sites displacement and on the angular limit of their bonding, if described in terms of K_G^F parameters. The only number of sites in a molecule plays a role in this case. It is also worth noting that such an approximation eliminates any temperature dependence since the direct connection with the square well potential (3) is broken. In order to recover the temperature dependence we should interrelate the values K_G^F with the

square well parameters E_G^F of the initial potential. Within the second virial coefficient approximation the relationship required is given by ref. 29

$$\sum_{F,G} K_G^F = \sum_{F,G} \Delta_G^F [\exp\{\beta E_G^F\} - 1] = \Delta \left[\exp\left\{\frac{1}{T^*}\right\} - 1 \right] \tag{39}$$

The value $T^* = 1/\beta^*$ is the dimensionless measure of temperature. The constant Δ_G^F arises after the averaging over orientations. This value depends on the displacement of the sites inside the molecule and also on the angular limit for the site–site bonding. For the case of water-like tetrahedral symmetry Δ_G^F is analytically calculated.[33, 25] We, therefore, conclude that the temperature properties of a fluid with arbitrary geometry of the sites displacement could be recovered through the above scheme, but with the precision of the second virial coefficient. It was shown[28] that such an approximation is reasonable for a quantitative description at not too low temperatures. In particular, the relation (39) is shown to be appropriate for a description of density profiles and adsorption isotherms for the model in contact with a hard wall. As follows from a comparison with computer simulation data,[26] Eq. (39) is applicable at any T^* for high densities, but becomes only qualitatively correct with decreasing density and temperature.

The expressions for the partial densities within the sticky limit are derived in refs. 25, 27. In particular, the X_A is defined by

$$X_A = \frac{\sqrt{1 + 32\pi K y_{00}^{00}(d)\,\rho} - 1}{16\pi K y_{00}^{00}(d)\,\rho} \tag{40}$$

where $y_{00}^{00}(d)$ is the contact value of the cavity correlation function for nonbonded molecules.

The OZ-like equation (30) together with the PY-like closure conditions (32), (33) and relation between the densities form a closed set of equations to be solved. The method proposed for its solution is based upon Wertheim–Baxter (WB) factorization technique,[35, 36] which allows one to express the connectivity functions through the auxiliary factorizing q-functions.

$$rh_{ij}^{\dagger}(r) = -[q_{ij}^{\dagger}(r)]' + 2\pi \sum_{nk} \int_0^1 q_{in}^{\dagger}(t)\,\sigma_{nk} h_{kj}^{\dagger}(|r-t|)(r-t)\,dt \tag{41}$$

$$rc_{ij}^{\dagger}(r) = -[q_{ij}^{\dagger}(r)]' + 2\pi \sum_{nk} \frac{\partial}{\partial r} \left(\int_0^1 q_{ni}^{\dagger}(t)\,\sigma_{nk} q_{kj}^{\dagger}(r+t)\,dt \right) \tag{42}$$

where the prime denotes the differentiation with respect to r. The auxiliary WB-factor functions within the PY approximation have the property that

$$q_{ij}^{\dagger} = 0, \qquad \text{for} \quad r < 0 \quad \text{and} \quad r > d \tag{43}$$

The q-functions at $0 < r < d$ can be obtained now from Eq. (41) utilizing the relations (34) and (35) within the limit (38). As result we get

$$q_{ij}^{\dagger}(r) = \delta_{ij} K y_{00}^{00}(d) \tag{44}$$

5. RESULTS AND DISCUSSION

The mean cluster size for a spatially homogeneous system is given by

$$S = 1 + \rho \int d\mathbf{r}\, g^{\dagger}(r) = 1 + \rho \lim_{k \to 0} \hat{g}^{\dagger}(k) \tag{45}$$

where $\hat{g}^{\dagger}(k)$ denotes the Fourier transform of $g^{\dagger}(r)$. Calculating the partial Fourier transforms $\hat{g}_{ij}^{\dagger}(k)$ from equation (30) we get the total $\hat{g}^{\dagger}(k)$ in terms of partial $\hat{c}_{ij}^{\dagger}(k)$. Then the mean cluster size can be expressed through the q-functions as

$$S = 1 + 8\rho X_A^2 \lim_{k \to 0} \{ [(\mathbf{q}(\mathbf{k}) * \boldsymbol{\sigma} * \mathbf{q}^{\mathrm{T}}(-\mathbf{k}))^{-1} - \boldsymbol{\sigma}]_{00} + [(\mathbf{q}(\mathbf{k}) * \boldsymbol{\sigma} * \mathbf{q}^{\mathrm{T}}(-\mathbf{k}))^{-1} - \boldsymbol{\sigma}]_{10} \} \tag{46}$$

where the Fourier transform is defined as

$$q_{ij}^{\dagger}(k) = [\boldsymbol{\sigma}^{-1}]_{ij} - 2\pi \int_0^{\infty} q_{ij}^{\dagger}(r) \exp(-ikr)\, dr \tag{47}$$

Performing the above calculation we get

$$S = 1 + \frac{32\pi\rho X_A^2 K y_{00}^{00}(d)(1 - 6\pi\rho X_A^2 K y_{00}^{00}(d))}{(1 - 12\pi\rho X_A^2 K y_{00}^{00}(d))^2} \tag{48}$$

The mean cluster size as a function of density is plotted in Fig. 1a. one can see that S has a singularity point $\eta_p (\eta = \pi\rho\, d^3/6)$ which depends on the temperature:

$$\eta_p = \frac{3\eta}{2} [1 - X_A]$$

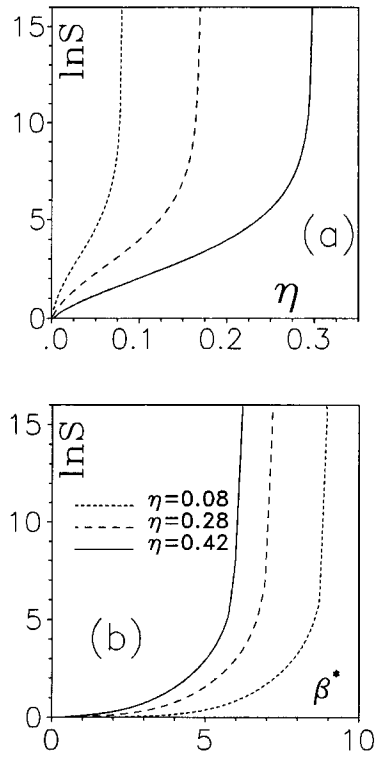

Fig. 1. (a) ln S as a function of density at different β^*: $\beta^* = 7$ (solid), $\beta^* = 8$ (long dashed), $\beta^* = 9$ (short dashed) (b) ln S as a function of β^* at different η.

Near the singularity the expression (48) can be rearranged to the following asymptotic form $S \propto (\eta - \eta_p)^{-\gamma}$. We thus conclude that the critical exponent γ describing the singularity in S is equal 2. Note that the same value of γ is obtained for other potential models of percolation.[5–9, 12–16] As is seen at the Fig. 1b the S increases with decreasing temperature. The inverse temperature β_p^* of the percolation transition diminishes with increasing density since the mean cluster size increases with η.

The mean cluster size can also be expressed in terms of X_A as

$$S = \frac{4(4 + X_A - 2X_A^2)}{3(1 - 6X_A + 9X_A^2)} \tag{49}$$

The above expression derived within the percolation theory is different from that obtained by Ghonasgi and Chapman[25] on the basis of the

thermodynamic perturbation theory (TPT) ignoring the branched polymers

$$S=\frac{3X_A^3-3X_A^2+1}{X_A^4(1-X_A^2+X_A^3)} \tag{50}$$

Our result for S is also different from the one obtained by Chapman *et al.*[30] under the constraint that the rings are ignored

$$S=\frac{1}{2X_A-1} \tag{51}$$

The correspondent curves are depicted in Fig. 2. As is seen, the result of (50) (the long dashed curve) is in excellent agreement with the MC data for high X_A. This is due to the use of TPT which is correct at high temperatures (i.e. when $X_A \to 1$). Our result (49) overestimates the cluster size at intermediate X_A but coincides with (50) at high X_A. This is due to the PY approximation used for calculation of S. Nevertheless, equation (50) predicts $S \to \infty$ when $X_A \to 0$. i.e. at zero temperature (as is depicted in Fig. 3), while (49) gives the percolation transition at finite temperatures. The prediction of (51) (the short dashed line) exhibits a singularity at $X_A = 1/2$ but S is not defined for $X_A < 1/2$. Therefore, both equations (49) and (51) predict the percolation threshold at finite temperatures. In order to determine which of these predictions is correct, computer simulations, carried out at low temperatures, are required. Note in addition that the region where $X_A < 1/3$ corresponds in our case to the percolating half-plane (see Fig. 4a). The cluster size is infinite for this region and predictions of Eq. (49) are, therefore, unphysical for $X_A < 1/3$. The latter fact is due to the

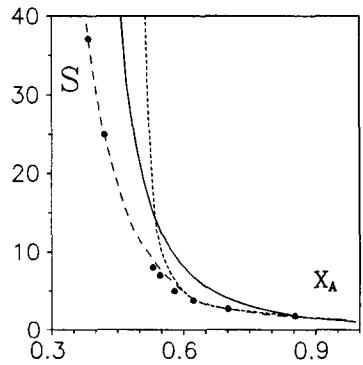

Fig. 2. Mean cluster size as a function of X_A: the present theory (solid), the result of Eq. (50) (long dashed), the result of Eq. (51) (short dashed), the MC data of ref. 25 (points).

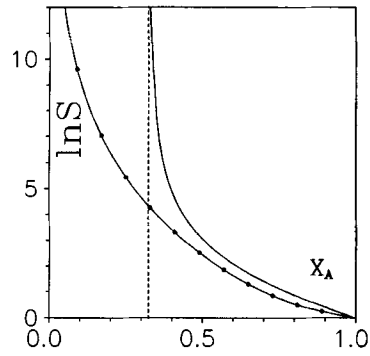

Fig. 3. $\ln S$ as a function of X_A near the threshold: present theory (solid), the result of Eq. (50) (dotted solid). The dashed line marks the percolation threshold.

ideal network approximation which is only qualitatively correct at low temperatures i.e. in the region where X_A is low. Physically, this means that the network, in our case, is described to remain only singly connected at any temperature. This approximation may become inadequate at low temperatures when the associative bonds cause the formation of additional connectivity pathes.

The percolation threshold is determined by analysing the conditions for the divergence of S. It is seen that $S \to \infty$ when $X_A \to 1/3$. Analysis of this condition allows us to obtain the percolation curve and to define the percolating and non-percolating regions. The percolation and spinodal[27] curves are given in Fig. 4a.

As follows from Fig. 4a the percolation temperature T^* increases with increasing density. We observe that the region of "normal" liquid states is inside the percolating region. This fact allows us to conclude that a liquid appears in the model as an infinite network. The conclusion is consistent with those drawn for the lattice models[22–24] and also within the primitive model of water.[33] In particular, we can state that the liquid phase occures when an infinite network is modified with decreasing temperature or increasing density. The percolation and spinodal curves do not meet at critical point. This result is in agreement with those obtained for spherically symmetric attraction models.[5–7]

It worth noting that the system is thermodynamically stable, since the Helmholtz free energy[19, 25] remains finite as X_A changes from 1 to 0 with decreasing temperature. In this way the free energy changes from that of hard sphere fluid to that of a four-fold coordinated network. This is in contrast to the Baxter's model, which is shown[34] to be thermodynamically unstable since the adhesive singular potential leads to the unsaturable

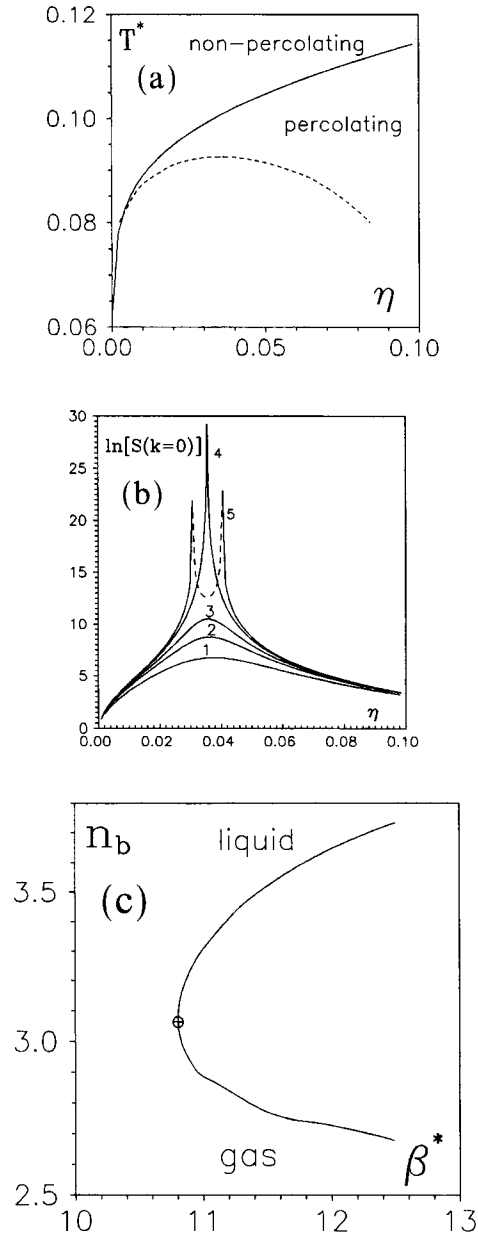

Fig. 4. (a) The spinodal (dashed) and percolation (solid) curves obtained within the ideal network approximation. (b) $\ln S(k=0)$ as a function of density for different K: (1) $k=6$; (2) $K=7.2$; (3) $k=7.4$; (4) $k=7.692$ (critical); (5) $K=7.8$ (supercritical). (c) the average number of bonds per molecule, calculated along the spinodal curve, as a function of β^*.

clustering. In our case the association is saturable and the clusters grow keeping the average member of bonds per molecule $n_b \leqslant 4$. Another evidence of thermodynamical stability is that the range of instability can be properly determined. This is illustrated by analysis of the isothermal compressibility χ_T, determined in ref. 27 in terms of $k \to 0$ limit of the structure factor $S(k)$. In Fig. 4b a plot of $\ln S(k=0)$ vs η is shown. The range of instability is shown in dashed curve. In the case of Baxter's model there is no real solution in this place and the spinodal curve is obtained as a boundary at which the solutions become complex.

The average member of bonds per molecule given by Eq. (29) is $n_b = 2.67$ at the transition. This value is confined between $n_b = 1.53$ (obtained for the bond percolation within the ST2 model of water[24]) and $n_b = 3.18$ (obtained for the percolation of four-fold patches).[24] The fractions of molecules bonded at n sites are

$$\chi_0 = 0.012, \qquad \chi_1 = 0.097, \qquad \chi_2 = 0.29, \qquad \chi_3 = 0.39, \qquad \chi_4 = 0.19$$

at the threshold. We thus see that the network consists mainly of two- and three-fold coordinated molecules at the percolation transition. We note that the percolation threshold obtained here ($X_A = 1/3$) is higher than $p = 1/3$ detected by Kolafa and Nezbeda[32] for primitive model of water (X_A corresponds to $1 - p$ in their notations). This is due to the fact that the threshold in ref. 32 is determined within the Cayley tree approximation with p being a random variable. In our case the structure is similar to the Cayley tree, but includes additional backbones which are irrelevant to the connectivity. The percolation threshold is, therefore, higher then at the Cayley tree.

We have calculated the value of n_b as a function of inverse temperature β^* along the spinodal curve, this plot is given in Fig. 4b. It is seen that the average member of bonds per molecule $n_b \approx 3.05$ at the critical point. Therefore, the condensation of a network fluid corresponds to increasing n_b from $n_b = 2.67$ to $n_b = 3.05$. One can conclude also that along the spinodal n_b increases with decreasing temperature at the liquid subbranch. Along the gaseous subbranch n_b decreases with decreasing temperature. In other words, a restriction on n_b is required in order to omit the gas-liquid coexistence region.

To calculate the connectivity correlation functions we use the Perram's iterative procedure.[37] As a starting point, the contact values $h_{ij}^{\dagger}(d^+)$ are needed. They are derived from Eq. (41) after putting $r = d$

$$h_{ij}^{\dagger}(d^+) = 4\pi\rho X_A^2 [y_{00}(d)\, K]^2 (\delta_{ij} + 1) \tag{52}$$

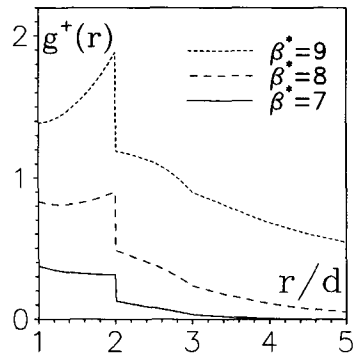

Fig. 5. Pair connectedness function at $\eta = 0.08$ for different values of β^*.

The total contact value $h^{\dagger}(d^+)$ given by

$$h^{\dagger}(d^+) = \left[\frac{m-1}{m}\right]^2 \frac{1}{4\eta} = [1 - X_A]^2 \frac{1}{4\eta} \tag{53}$$

describes the contact probability of two molecules in the same cluster. Note that $h^{\dagger}(d^+)$ is inversly proportional to the density η which indicate the increasing of the intracluster correlation at low densities. It is seen also that the contact probability at a given density is highest at $X_A = 0$, i.e. when the system consists mainly of highly coordinated molecules. We conclude, therefore, that at the percolation threshold ($X_A = 1/3$) the contact probability is not maximal, which is consistent with $n_b = 2.67$ for an infinite cluster.

The connectivity correlation functions for $\eta = 0.08$ at verious β^* are plotted in Fig. 5. One can observe how $h^{\dagger}(r)$ becomes increasingly long

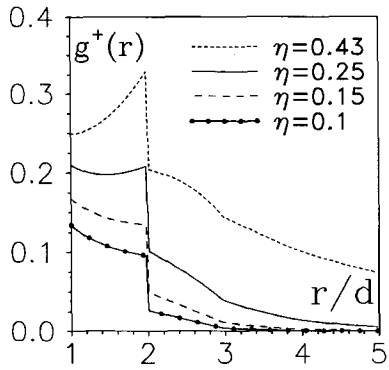

Fig. 6. Pair connectedness function at $\beta^* = 6$ for different values of η.

ranged as the percolation threshold is approached. As follows from the Fig. 6, this tendency remains unchanged for a fixed temperature $\beta^* = 6$ with η increasing up to the threshold. As expected all the curves decrease as r is increased and are discontinuous at $r = 2d$. This implies that the excluded-volume interaction between the particles belonging to the same cluster is not prominant.

6. CONCLUSION

In this paper we reformulate the Wertheim's integral equation theory in order to study the connectivity properties of a four bonding sites fluid. We adapt the ideal network approximation which describes the network as an infinite cluster with only single path of associative bonds between any pair of molecules. We calculate the mean cluster size and pair connectedness functions within the PY approximation from the OZ connectivity integral equation. It is shown that the mean cluster size increases with increasing density as well as with decreasing temperature and become infinite as the percolation threshold is approached. Based on this we define the percolation curve and percolating region of temperature and density. The threshold is displayed to be higher than at the Cayley tree, since the network in our case is a Cayley tree with additional deadlock branches. It is shown that a region of "normal" liquid states is inside the percolation region if both are detected within the ideal network approximation. The pair connectedness functions are detected to become increasingly long ranged as the percolation threshold is approached.

REFERENCES

1. D. Stauffer, *Introduction to Percolation Theory* (Taylor & Francis, London, 1985).
2. P. G. de Gennes, *Scaling Concepts in Polymer Physics*, Cornell University Press, Ithaca, NY, 1979.
3. S. A. Safran, I. Webman, and G. S. Grest, *Phys. Rev. E* **32**:506 (1985).
4. A. Coniglio, U. de Angelis, and A. Forlani, *J. Phys. A* **10**:1123 (1977).
5. Y. C. Chiew and E. D. Glandt, *J. Phys. A* **16**:2599 (1983).
6. Y. C. Chiew, G. Stell, and E. D. Glandt, *J. Chem. Phys.* **83**:761 (1985).
7. G. Wu and Y. C. Chiew, *J. Chem. Phys.* **90**:5024 (1989).
8. S. Maran and L. Reatto, *J. Chem. Phys.* **89**:5038 (1988).
9. T. DeSimone, S. Demoulini, and R. M. Stratt, *J. Chem. Phys.* **85**:391 (1986).
10. J. Xu and G. Stell, *J. Chem. Phys.* **89**:1101 (1988).
11. Y. C. Chiew and Y. H. Wang, *J. Chem. Phys.* **89**:6385 (1988).
12. A. O. Weist and E. D. Glandt, *J. Chem. Phys.* **95**:8365 (1991), **97**:4316 (1992).
13. M. Holovko and J. P. Badiali, *Chem. Phys. Lett.* **204**:511 (1993).
14. G. Cassin, Yu. Duda, M. Holovko, J. P. Badiali, and M. Pileni, *J. Chem. Phys.* (in press).
15. D. Laria and F. Vericat, *Phys. Rev B.* **40**:353 (1989).

16. K. Leung and D. Chandler, *J. Stat. Phys.* **63**:837 (1991).
17. A. O. Weist and E. D. Glandt, *J. Chem. Phys.* **101**:5167 (1994).
18. M. S. Wertheim, *J. Stat. Phys.* **35**:19, 35 (1984).
19. M. S. Wertheim, *J. Stat. Phys.* **42**:459, 477 (1986).
20. M. S. Wertheim, *J. Chem. Phys.* **85**:2929 (1986).
21. M. S. Wertheim, *J. Chem. Phys.* **87**:73 (1987).
22. H. E. Stanley and J. Teixeira, *J. Chem. Phys.* **73**:3404 (1980).
23. H. E. Stanley, J. Teixeira, A. Geiger, and R. L. Blumberg, *Physica* **106A**:260 (1981).
24. R. L. Blumberg, H. E. Stanley, A. Geiger, and P. Mausbach, *J. Chem. Phys.* **80**:5230 (1984).
25. D. Ghonasgi and W. G. Chapman, *Mol. Phys.* **79**:291 (1993).
26. C. J. Segura and W. G. Chapman, *Mol. Phys.* **86**:415 (1995).
27. E. Vakarin, Yu. Duda, and M. F. Holovko, *Mol. Phys.* **90**:613 (1997).
28. E. Vakarin, Yu. Duda, and M. F. Holovko, *Mol. Phys.* **90** (1997) (in press).
29. G. Jackson, W. G. Chapman, and K. Gubbins, *Mol. Phys.* **65**:1 (1988).
30. W. G. Chapman, G. Jackson, and K. E. Gubbins, *Mol. Phys.* **65**:1057 (1988).
31. J. Chang and S. Sandler, *J. Chem. Phys.* **102**:437; **103**:3196 (1995).
32. J. Kolafa and I. Nezbeda, *Mol. Phys.* **72**:777 (1991).
33. I. Nezbeda and G. A. Iglesias-Silva, *Mol. Phys.* **69**:767 (1990).
34. G. Stell, *J. Stat. Phys.* **63**:1203 (1991).
35. M. S. Wertheim, *J. Math. Phys.* **5**:643 (1964).
36. R. J. Baxter, *J. Chem. Phys.* **49**:2770 (1968).
37. J. W. Perram, *Mol. Phys.* **30**:1505 (1975).